

# Direct Electrochemistry and Electrocatalysis Behaviors of Glucose Oxidase Based on Hyaluronic Acid-Carbon Nanotubes-Ionic Liquid Composite Film

Shangguan, Xiaodong(上官小东) Zheng, Jianbin\*(郑建斌)  
Zhang, Hongfang(张宏芳) Tang, Hongsheng(汤宏胜)

*Institute of Analytical Science/Shaanxi Provincial Key Laboratory of Electroanalytical Chemistry,  
Northwest University, Xi'an, Shaanxi 710069, China*

Multi-walled carbon nanotubes (MWNTs) were dispersed in the ionic liquid [BMIM][BF<sub>4</sub>] to form a uniform black suspension. Based on it, a novel glucose oxidase (GOx)-hyaluronic (HA)-[BMIM][BF<sub>4</sub>]-MWNTs/GCE modified electrode was fabricated. UV-vis spectroscopy confirmed that GOx immobilized in the composite film retained its native structure. The experimental results of EIS indicated MWNTs, [BMIM][BF<sub>4</sub>] and HA were successfully immobilized on the surface of GCE and [BMIM][BF<sub>4</sub>]-MWNTs could obviously improve the diffusion of ferricyanide toward the electrode surface. The experimental results of CV showed that a pair of well-defined and quasi-reversible peaks of GOx at the modified electrode was exhibited, and the redox reaction of GOx at the modified electrode was surface-confined and quasi-reversible electrochemical process. The average surface coverage of GOx and the apparent Michaelis-Menten constant were  $8.5 \times 10^{-9}$  mol/cm<sup>2</sup> and 9.8 mmol/L, respectively. The cathodic peak current of GOx and the glucose concentration showed linear relationship in the range from 0.1 to 2.0 mmol/L with a detection limit of 0.03 mmol/L (*S/N*=3). As a result, the method presented here could be easily extended to immobilize and obtain the direct electrochemistry of other redox enzymes or proteins.

**Keywords** analytical methods, nanotubes, electroanalysis, ionic liquids, glucose oxidase, hyaluronic acid

## Introduction

Direct electrochemistry behavior of redox proteins is important for the research of their metabolic processes and construction of the biosensors and bioreactors. However, the direct electron transfer between proteins and bare solid electrode is difficult because the electroactive centers of the protein are deeply embedded in the protein structure, as well as adsorptive denaturation and unfavorable orientations of proteins onto electrode surfaces.<sup>1</sup> Hence, different biocompatible immobilizing materials, including polymer,<sup>2,4</sup> silica sol-gel film,<sup>5</sup> polyacrylamide microgel matrix, *etc.*,<sup>6</sup> are used to promote the electron transfer. It has been demonstrated to be very effective in preparing amperometric biosensors.<sup>7,8</sup>

Carbon nanotubes (CNTs) possess many unique mechanical electronic properties, high chemical stability and high surface-to-volume ratio *etc.* Of them, their biocompatibility and ability to facilitate electron transfer make them suitable candidates for the direct electrochemistry of enzymes.<sup>9-13</sup> In most cases, the direct electrochemistry of protein/enzyme was carried out based on the synergic effect of CNTs and other biocompatible

materials. Glucose biosensors were successfully fabricated by glucose oxidase (GOx) immobilized within the CNTs and chitosan composite film,<sup>14</sup> on the quantum dots/carbon nanotubes electrode,<sup>15</sup> in sol-gel composite plane pyrolytic graphite electrode modified with CNT,<sup>16</sup> on the boron-doped CNTs modified electrode.<sup>17</sup>

In recent years, ionic liquids (ILs), as supporting electrolyte and modifier, have been applied to studying direct electrochemistry of redox proteins.<sup>18</sup> Enzymes are usually active and protein refolding is improved in ILs.<sup>19-25</sup>

Immobilization of redox proteins is significant step in constructing biosensors or bioreactors.<sup>26</sup> Biocompatible materials have been used widely by entrapment or encapsulation of proteins within them to realize direct electrochemistry of redox proteins for their desirable properties, such as nontoxic and biocompatible, and potential applications for the fabrication of biosensors.<sup>27</sup> Among various biocompatible materials, hyaluronic acid (HA), ubiquitously distributed in the extracellular spaces, is a linear polysaccharide built from repeating disaccharide units ([*D*-glucuronic acid (1- $\beta$ -3) *N*-acetyl-*D*-glucosamine (1- $\beta$ -4)]<sub>*n*</sub>) of molecular weight

\* E-mail: zhengjb@nwu.edu.cn; Tel.: 0086-029-88302077; Fax: 0086-029-88303448

Received March 17, 2010; revised May 12, 2010; accepted June 2, 2010.

Project supported by the National Natural Science Foundation of China (Nos. 20875076, 20905061) and the Research Fund for the Doctoral Program of Higher Education (No. 20060697013).

$10^4$ – $10^7$  Daltons.<sup>28</sup> Since HA is a naturally occurring biopolymer, it is biocompatible and biodegradable,<sup>29</sup> and it has been utilized as an immobilization matrix for biosensors and biocatalysis.<sup>30–33</sup>

The present paper focused on (1) multi-walled carbon nanotubes (MWNTs) dispersed in the [BMIM][BF<sub>4</sub>]; (2) preparation and characterization of the different composite by UV-vis spectrum, electrochemical impedance spectroscopy (EIS) and cyclic voltammetry (CV); (3) hindrance of HA for GOx-[BMIM][BF<sub>4</sub>]-MWNTs leaking from the electrode surface; (4) electrochemical response of the different electrodes; (5) synergistic effects of the HA-[BMIM][BF<sub>4</sub>]-MWNTs system. The preliminary analytical performance of the HA-GOx-[BMIM][BF<sub>4</sub>]-MWNTs film electrode for glucose was evaluated as well.

## Experimental

### Chemicals

GOx (E.C. 1.1.3.4, 182 U/mg, Type X-S from *Aspergillus niger*) and HA (Mr 1500 kDa) were purchased from Sigma (USA). MWNTs (diameter: 10–20 nm, length: 5–15 μm, purity: ≥98%, special surface area: 40–300 m<sup>2</sup>/g) came from Shenzhen Nanotech Port Co. Ltd. (Shenzhen, China). [BMIM][BF<sub>4</sub>] was synthesized and purified following the similar procedures described in the literature.<sup>34</sup> K<sub>4</sub>Fe(CN)<sub>6</sub>, K<sub>3</sub>[Fe(CN)<sub>6</sub>] and β-D(+)-glucose were of analytical grades and used without further purification. 0.1 mol/L phosphate buffer solution (PBS) was used as the supporting electrolyte. Solution pH values were adjusted by 0.1 mol/L phosphoric acid solution and 0.1 mol/L sodium hydroxide solution. All other reagents were of analytical grade and used without further purification. All aqueous solutions were made with deionized water.

### Apparatus

A model CHI660A electrochemical workstation (Shanghai Chenhua Co. Ltd, China) controlled by a microcomputer with CHI660A software was employed for all electrochemical measurements in the experiment. DL-180 ultrasonic cleaning machine (35 kHz, Zhejiang Haitian Electron Instrument Factory, China) was used to dissolve and form homogeneous solution. A three-electrode system, where a standard saturated calomel electrode (SCE) served as the reference electrode, a platinum wire electrode as the auxiliary electrode and the prepared electrodes as the working electrode. Ultraviolet-visible (UV-vis) spectra were obtained on a Lambda 40 UV-vis spectrophotometry (Perkin Elmer Instrument Co. Ltd., USA). All potentials reported were versus the SCE.

### Electrode preparation

Before modification, glassy carbon electrode (GCE) (diameter: 3.0 mm) was polished with 1.0, 0.3 and 0.05 μm alumina slurry, respectively. Then, the electrode

was ultrasonicated in ethanol, acetone and deionized water bath, and dried in air.

The MWNTs was purified through refluxing in HNO<sub>3</sub>-H<sub>2</sub>SO<sub>4</sub> (volume ratio, 1 : 1) mixture, washed with redistilled water and dried under vacuum. [BMIM][BF<sub>4</sub>]-MWNTs was prepared as follows: MWNTs were dispersed in [BMIM][BF<sub>4</sub>] to form a uniform black suspension (1.0 mg/mL) with the aid of ultrasonics 30 min. After that, a homogeneous solution containing 1.0 mg/mL HA, 10 mg/mL GOx, and 5% ( $V_{\text{MWNTs-IL}}/V_{\text{Total}}$ ) [BMIM][BF<sub>4</sub>]-MWNTs was prepared by adding an appropriate volume of HA solution, GOx solution and [BMIM][BF<sub>4</sub>]-MWNTs into 0.1 mol/L PBS (pH 7.0). Then 10 μL of this homogeneous solution was cast onto the electrode surface by using a syringe to prepare GOx-HA-[BMIM][BF<sub>4</sub>]-MWNTs. A beaker was covered over the electrode so that water could evaporate slowly in air and a uniform film could be formed. The dried HA-GOx-[BMIM][BF<sub>4</sub>]-MWNTs was stored at 4 °C in a refrigerator when not in use. The HA/GCE, HA-MWNTs/GCE, GOx-HA-MWNTs/GCE, GOx-HA/GCE and HA-MWNTs-[BMIM][BF<sub>4</sub>]/GCE modified electrodes were prepared in the same way.

### Experimental procedure

The electrochemical measurements were carried out in 20 mL cells containing 0.1 mol/L PBS (pH 7.0). Prior to measurement, PBS was deaerated with nitrogen gas stream for 30 min, and then a nitrogen atmosphere was maintained over the cell during the experiments. When the proper amount of glucose was transferred into cell, the experiment was performed in the 0.1 mol/L aerated PBS (pH 7.0). The three-electrode system was immersed into the solution.

CV experiment was performed between –1.0 and 0 V. The peak currents and potentials were recorded by CHI660A workstation. UV-Vis spectra measurements were recorded on a Lambda 40 UV-Vis spectrophotometry with wavelength scope of 210–500 nm. Electrochemical impedance spectra (EIS) was performed in a solution of 1 mmol/L Fe(CN)<sub>6</sub><sup>3–/4–</sup> containing 0.1 mol/L KCl. The impedance measurements were recorded at a bias potential of +187 mV (vs. SCE) within the frequency range of 10<sup>5</sup>–10<sup>–2</sup> Hz. All the electrochemical experiments were conducted at room temperature.

## Results and discussion

### UV-vis spectra characterization

UV-Vis spectroscopy is a useful tool for giving structural information about the environmental surrounding of GOx. The Soret band of GOx would shift or disappear if GOx structure had been changed or denatured. Figure 1 showed the UV-Vis spectrum of HA, [BMIM][BF<sub>4</sub>], GOx and GOx-HA-[BMIM][BF<sub>4</sub>], respectively. HA (curve a) had no adsorption band in a

range of 250–500 nm. The spectrum of [BMIM][BF<sub>4</sub>] (curve b) exhibited a peak at 255 nm. The free GOx (curve c) showed two peaks for the characteristic of the oxidized form of flavin groups at about 380 and 450 nm.<sup>35</sup> The position and shape of adsorption bands (380 and 450 nm) for GOx in HA-[BMIM][BF<sub>4</sub>] composite (curve d) were almost the same as those for free GOx, suggesting that the chromophoric groups of flavin adenine dinucleotide (FAD) responsible for the GOx visible adsorption spectrum should be embedded in the GOx polypeptide matrix and did not come out of the pockets during the process of immobilization of GOx by HA-[BMIM][BF<sub>4</sub>]. Moreover, a close inspection of the spectrum of free GOx and the GOx-HA-[BMIM][BF<sub>4</sub>] at about 275 nm in both the cases is due to the e-e\* transitions arising from the tryptophan and tyrosine residues on the enzyme surface.<sup>36</sup> It might provide that the GOx immobilized on HA-[BMIM][BF<sub>4</sub>] indeed maintained its native structure.

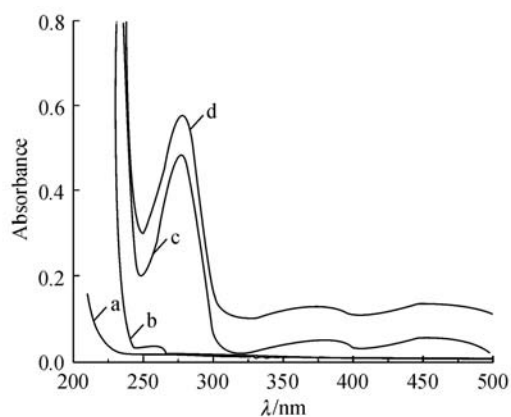


**Figure 1** UV-visible absorption spectra of HA solution (a), [BMIM][BF<sub>4</sub>] (b), GOx solution (c) and HA-[BMIM][BF<sub>4</sub>]-GOx solution (d).

### Characterization of biocomposite material

EIS is an effective method to probe the features of surface-modified electrodes<sup>37</sup> and provide the useful information on the impedance changes of the modified electrode surface.<sup>38</sup> The curve of EIS includes a semi-circular part and a linear part. The semicircular part locating at higher frequency, which controls the electron transfer kinetics of the redox probe at the electrode interface, corresponds to the electron transfer limited process and the electron transfer resistance ( $R_{et}$ ) can be attained by its diameter. Meanwhile, the linear part locating at lower frequency affords the information on the diffusion process in solution. Figure 2 exhibited the EIS of the bare GCE (curve a), HA-[BMIM][BF<sub>4</sub>]-MWNTs/GCE (curve b), HA-MWNTs/GCE (curve c) and HA/GCE (curve d) in a mixture solution of 1 mmol/L Fe(CN)<sub>6</sub><sup>3-/4-</sup> (1 : 1) containing 0.1 mol/L KCl. On the bare GCE,  $R_{et}$  could be estimated to be 353 Ω. The semicircle of the HA/GCE increased dramatically and

the  $R_{et}$  was 5.65 kΩ, which indicated that HA film was an obstacle making the electron transfer of interface more difficult. When the HA-MWNTs was immobilized onto GCE, the  $R_{et}$  decreased to 3.94 kΩ, resulting from the conductivity of MWNTs, which indicated that MWNTs were successfully immobilized on the surface of GCE. When HA-[BMIM][BF<sub>4</sub>]-MWNTs film was anchored on the GCE, the electron transfer resistance decreased dramatically to 1.41 kΩ, which could be ascribed to the high conductivity of [BMIM][BF<sub>4</sub>]. All mentioned above indicated [BMIM][BF<sub>4</sub>], MWNTs and HA were successfully immobilized on the surface of GCE and [BMIM][BF<sub>4</sub>]-MWNTs could obviously improve the diffusion of ferricyanide toward the electrode surface.

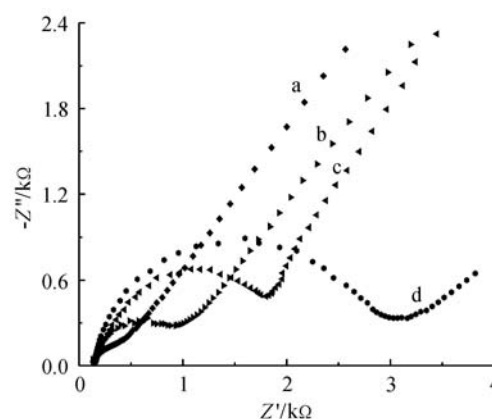


**Figure 2** Electrochemical impedance spectroscopy for bare GCE (a), HA-MWNTs-[BMIM][BF<sub>4</sub>]/GCE (b), HA-MWNTs/GCE (c) and HA/GCE (d) in a solution of 1 mmol/L Fe(CN)<sub>6</sub><sup>3-/4-</sup> + 0.1 mol/L KCl as the supporting electrolyte. The frequencies swept from 10<sup>5</sup> to 10<sup>-2</sup> Hz.

The electrochemical behaviors of different modified electrodes were characterized by 1.0 mmol/L Fe(CN)<sub>6</sub><sup>3-</sup> solution containing 0.1 mol/L KCl at 100 mV/s and the cyclic voltammograms were shown in Figure 3. Curve a was the voltammetric response of redox behavior of Fe(CN)<sub>6</sub><sup>3-</sup> at the bare GCE. A pair of quasi-reversible and well-defined redox peaks could be observed at the bare GCE with 80 mV of the peak-to-peak separation ( $\Delta E_p$ ) (curve a), indicating a fast and direct electron transfer reaction occurred. After casting the HA on the bare GCE, both the cathodic and anodic peak currents decreased obviously and the  $\Delta E_p$  increased to 146 mV (curve b). It indicated that the HA film could act as the inert electron and mass transfer blocking layer, which hindered the diffusion of Fe(CN)<sub>6</sub><sup>3-</sup> toward the electrode surface. When HA-MWNTs was immobilized on bare GCE, the peak currents of Fe(CN)<sub>6</sub><sup>3-</sup> increased with 137 mV of  $\Delta E_p$  (curve c), which showed that MWNTs could be immobilized on the GCE surface successfully and promote the electron transfer between the Fe(CN)<sub>6</sub><sup>3-</sup> and the electrode surface. When HA-[BMIM][BF<sub>4</sub>]-MWNTs was cast on bare GCE, the peak

currents of  $\text{Fe}(\text{CN})_6^{3-}$  were restored close to the value obtained on a bare GCE with 105 mV of  $\Delta E_p$  (curve d). These results indicated that  $[\text{BMIM}][\text{BF}_4]\text{MWNTs}$  facilitates the electron transfer between the  $\text{Fe}(\text{CN})_6^{3-}$  and the electrode surface, and the presence of HA could successfully modify  $[\text{BMIM}][\text{BF}_4]\text{-MWNTs}$  on the GCE surface.

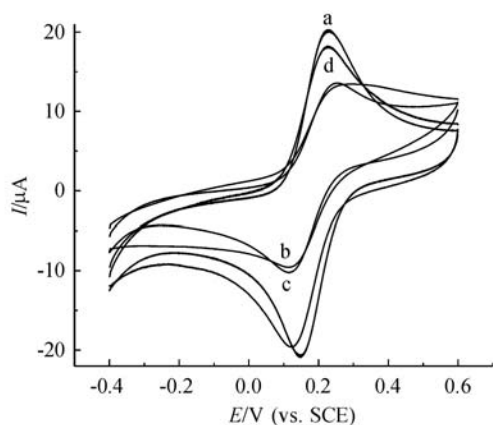


**Figure 3** The CV curves of bare GCE (a), HA/GCE (b), HA-MWNTs/GCE (c), HA-MWNTs-[BMIM][BF<sub>4</sub>]/GCE (d) in a solution of 1 mmol/L  $\text{Fe}(\text{CN})_6^{3-}$  containing 0.1 mol/L KCl at 100 mV/s.

### Direct electrochemistry of GOx

The direct electrochemistry of GOx at GOx-HA-[BMIM][BF<sub>4</sub>]-MWNTs/GCE was studied by CV. Figure 4 showed CV curves of different kinds of the modified GCE in 0.1 mol/L PBS (pH 7.0) at 200 mV/s. A pair of redox peaks of GOx was observed at GOx-HA/GCE (curve c). An enhanced electrochemical response of GOx was observed at GOx-HA-MWNTs/GCE (curve b) compared with curve c. It was possible that special surface and electron conductivity of MWNTs quickened electron transfer process between FAD of active redox centre of GOx and the surface of electrode. When the mixed solution of  $[\text{BMIM}][\text{BF}_4]\text{-MWNTs}$ , GOx and HA was cast on GCE, a remarkable enhanced electrochemical response of GOx was observed at GOx-HA-[BMIM][BF<sub>4</sub>]-MWNTs/GCE (curve a). The peak currents of GOx were four times as large as those of GOx-HA-MWNTs/GCE. A pair of well-defined, quasi-reversible redox peaks of GOx was appeared with  $-0.448$  V of oxidation potential ( $E_{pa}$ ),  $-0.504$  V of reduction potential ( $E_{pc}$ ),  $-0.476$  V of the formal potential  $E^{0'}$  [ $E^{0'} = (E_{pa} + E_{pc})/2$ ] and 56 mV of the  $\Delta E_p$ . Combined with UV-vis spectra, the result demonstrated that the electrochemistry response of GOx immobilized on the composite film was due to the redox of the prosthetic FAD bound to GOx, rather than free FAD.<sup>39</sup> HA-[BMIM][BF<sub>4</sub>]-MWNTs composite film could provide a favorable microenvironment for GOx to retain its natural structure and greatly enhance the electron transfer process between GOx and the basal electrode to realize its direct electrochemistry.

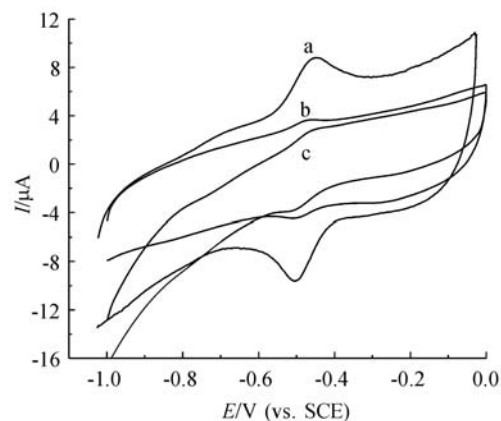


**Figure 4** The CV curves of HA-MWNTs-[BMIM][BF<sub>4</sub>]-GOx/GCE (a), HA-MWNTs-GOx/GCE (b) and HA-GOx/GCE (c) in 0.1 mol/L PBS (pH 7.0) at 200 mV/s.

Figure 5 was the CV curves of GOx-HA-[BMIM][BF<sub>4</sub>]-MWNTs/GCE in 0.1 mol/L PBS (pH 7.0) at different scan rates ( $v$ ) in a range from 50 to 600 mV/s. The results exhibited about symmetrical anodic and cathodic peaks of approximately equal heights for GOx at different scan rates. The peak currents ( $I_p$ ) were linearly with  $v$  in the range mentioned above in Figure 5 inset. The linear regression equation was  $I_{pa} (\mu\text{A}) = 0.471 + 0.0165v$  (mV/s),  $r = 0.9990$  ( $n = 18$ );  $I_{pc} (\mu\text{A}) = -1.53 - 0.0154v$  (mV/s),  $r = 0.9993$  ( $n = 18$ ), respectively. This indicated that the electron transfer process for GOx was a surface-confined process. The slope value of the logarithm of peak currents ( $\log I_p$ ) versus logarithm of scan rate ( $\log v$ ) for anodic and cathodic currents was very close to the theoretical value of 1 expected for thin layer electrochemical behavior.<sup>40</sup>

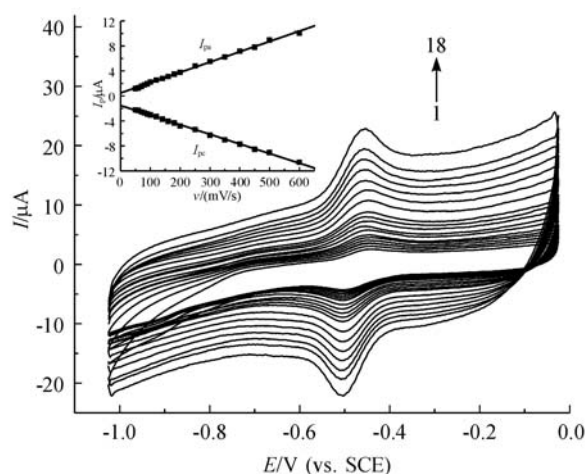


**Figure 5** The CV curves of HA-MWNT-[BMIM][BF<sub>4</sub>]-GOx/GCE in 0.1 mol/L PBS (pH 7.0) at different scan rate. Scan rate 1—18: 50, 60, 70, 80, 90, 100, 120, 140, 160, 180, 200, 250, 300, 350, 400, 450, 500, 600 mV/s. Inset is linear relationship of  $I_p$  and  $v$ .

According to the equation of  $I_p = n^2 F^2 v A \Gamma / 4RT = nFQv/4RT$ ,<sup>41</sup>  $Q$  is the charge involved in the reaction. A

is the geometric area of the modified GCE.  $n$  is the number of the electron transferred.  $F$  is the Faraday constant.  $\Gamma^*$  is the surface concentration of the electroactive substance.  $n$  was calculated as 1.91, meaning that  $2e$  transfer was involved.<sup>17</sup> At the same time, the  $I_{pa}/I_{pc} = 0.92 \approx 1$  and the  $E^0$  kept almost unchanged, which are the typical characteristics of a quasi-reversible system. So, the charge-transfer coefficient ( $\alpha$ ) was 0.5. According to the equation, the electron transfer rate constant ( $k_s$ ) was further estimated to be  $0.51 \text{ s}^{-1}$ ,<sup>42</sup> which was smaller than  $15.6 \text{ s}^{-1}$ .<sup>43</sup>

The average surface coverage ( $\Gamma$ ) of the electroactive GOx in the film was calculated to be  $8.5 \times 10^{-9} \text{ mol} \cdot \text{cm}^{-2}$  from the slope of the  $I_p$ - $v$  curve. This value was much larger than the literature value ( $2.86 \times 10^{-12} \text{ mol} \cdot \text{cm}^{-2}$ ),<sup>44</sup> suggesting that HA-MWNTs-[BMIM][BF<sub>4</sub>] provided a large area for enzyme immobilization.

#### Effects of HA, [BMIM][BF<sub>4</sub>]-MWNTs and pH value

The amount of HA was studied. When varying the HA amount from 0.5 to 1.5 mg/mL, stability of the peaks of GOx increased rapidly after successive potential scan with the increase of HA concentration. Considering that a large amount of HA could make the electron transfer of interface more difficult, 1.0 mg/mL HA was chosen as the appropriate amount to form composite film.

The effect of [BMIM][BF<sub>4</sub>]-MWNTs was also tested. The results showed that the peak current of GOx increased rapidly with the increase of [BMIM][BF<sub>4</sub>]-MWNTs and then levels off after 5% ( $V_{\text{MWNTs-IL}}/V_{\text{Total}}$ ) [BMIM][BF<sub>4</sub>]-MWNTs. Considering that a large amount of [BMIM][BF<sub>4</sub>]-MWNTs would increase the background current, 5% [BMIM][BF<sub>4</sub>]-MWNTs was chosen as the appropriate amount.

Cyclic voltammetric measurements of GOx-HA-[BMIM][BF<sub>4</sub>]-MWNTs/GCE showed a strong dependence on solution pH value. As could be seen from Figure 6, GOx exhibited a pair of stable and well-defined redox peaks in the range of pH value (3.92–7.90). Both anodic and cathodic peak potentials of GOx shifted to negative direction and the  $E^0$  versus pH gave a straight line (Figure 6 inset). The linear regression equation was  $E^0 = -0.122 - 0.051\text{pH}$ ,  $r = 0.9958$  ( $n = 4$ ). The slope was close to the theoretical value ( $-58.6 \text{ mV/pH}$ ,  $25^\circ \text{C}$ ) for a two-proton coupled with two-electron redox reaction process. Moreover, the solution pH values also affected the peak currents of the GOx-HA-[BMIM][BF<sub>4</sub>]-MWNTs/GCE. The maximum current response was observed when the solution pH value was 7.0. It might be due to that the immobilized GOx maintained its higher bioactivity at such a pH value.

#### Electrocatalytic activity of GOx at the modified electrode

The effect of the dissolved oxygen on the electrochemical behavior of the GOx-HA-[BMIM][BF<sub>4</sub>]-

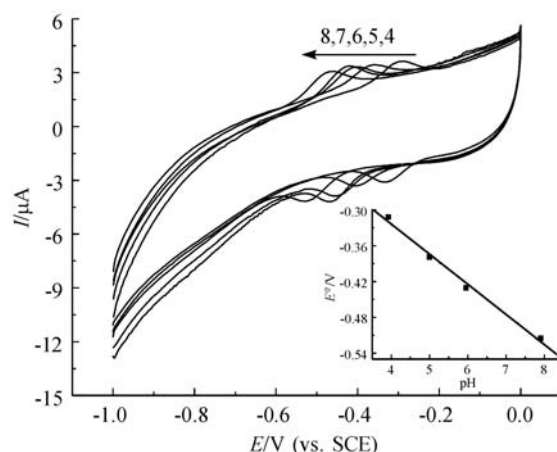


**Figure 6** The CV curves of HA-MWNTs-[BMIM][BF<sub>4</sub>]-GOx/GCE in 0.1 mol/L PBS with different pH value. Scan rate: 200 mV/s; solution pH: 3.92, 5.0, 5.95, 7.0 and 7.9 (from right to left). Inset: linear relationship of  $E^0$  and pH value.

MWNTs/GCE was investigated and the corresponding results are shown in Figure 7. A pair of well-defined, quasi-reversible redox peaks of GOx was observed in 0.1 mol/L both deoxygenated (curve a) and air-saturated (curve b) PBS (pH 7.0). However, the reduction peak current of GOx at the modified electrode in air-saturated PBS was larger than that in deoxygenated PBS and the oxidation peak current was in reverse. These changes demonstrated that GOx in the film nicely catalyzed the oxygen reduction according to Eqs. (1) and (2).<sup>44</sup> In other words, the assembled GOx retained its good catalytic activity.

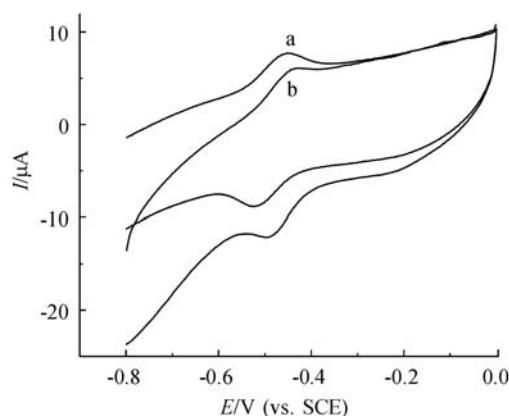
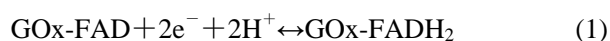


**Figure 7** The CV curves of the HA-MWNTs-IL-GOx/GCE in 0.1 mol/L deoxygenated (a) and air-saturated (b) PBS (pH 7.0) at 500 mV/s.



Moreover, with addition of glucose to air-saturated 0.1 mol/L pH 7.0 PBS, the reduction current decreased

from curve b to curve g in Figure 8. The higher glucose concentration was, the more reduction current decreased. This was potentially caused by the enzyme catalyzed reaction as follows:<sup>45</sup>

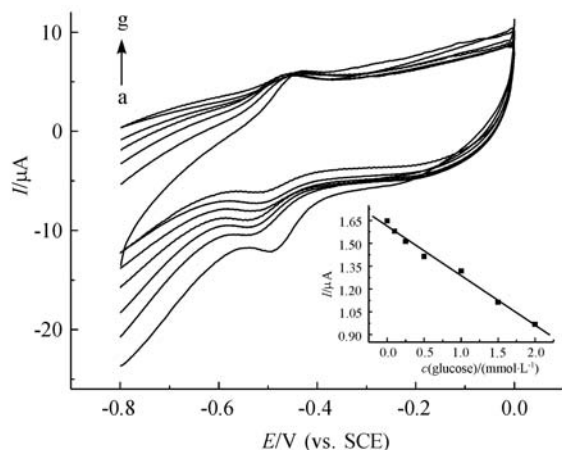
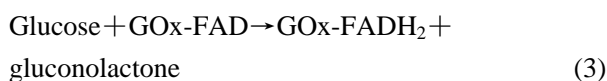


**Figure 8** The CV curves of of different concentration of glucose in 0.1 mol/L PBS (pH 7.0) at HA-MWNTs-[BMIM][BF<sub>4</sub>]-GOx/GCE at 500 mV/s. Concentration of glucose a–g: 0, 0.1, 0.25, 0.5, 1.0, 1.5, 2.0 mmol/L. Inset: linear relationship of  $I_{pc}$  and glucose concentration.

This trend can be explained that glucose is the substrate of GOx. When glucose was added to the air-saturated PBS, the enzyme-catalysis occurred and the oxidized form of GOx on electrode surface decreased. Thus, the addition of glucose restrained the electrocatalytic reaction and led to the decrease of reduction current. This could be employed to determine the glucose concentration.

Cathodic peak was occurred at about  $-0.53$  V in our experiments (Figure 8). The cathodic peak of GOx and the glucose concentration showed linear relationship in the ranges from 0.1 mmol/L to 2.0 mmol/L (Figure 8 inset). The linear regression equation was  $I_{pc}$  ( $\mu\text{A}$ ) =  $1.61 - 3.26C(\text{glucose})$  (mmol/L),  $r = 0.9947$  ( $n = 7$ ). The detection limit estimated was 0.03 mmol/L ( $S/N = 3$ ), which was larger than that obtained by using PEDOT-Pd/GOx-ME (0.075 mmol/L).<sup>46</sup>

The apparent Michaelis-Menten constant ( $K_m$ ), which gives an indication of the enzyme-substrate kinetics for the glucose biosensor, can be calculated from Lineweaver-Burk equation.<sup>47</sup> The corresponding plot yielded  $K_m$  of 9.8 mmol/L, which was smaller than 10.1 mmol/L for GOx-Au NP-CHIT,<sup>43</sup> 21 mmol/L for GOx-ZnO:Co nanoclusters,<sup>48</sup> 27 mmol/L for native GOx in solution,<sup>49</sup> 33 mmol/L at the GOx-DMF-CPE,<sup>50</sup> and 25.3 mmol/L at the GOx-polypyrrole,<sup>51</sup> suggesting that GOx immobilized on HA-MWNTs-BMIMBF<sub>4</sub>/GCE had good affinity to glucose. The good microenvironment due to synergistic effects of HA-[BMIM]-[BF<sub>4</sub>]-MWNTs system might contribute to the im-

provement of the affinity and good performances of the biosensor.

The sensitivity of the GOx-HA-[BMIM][BF<sub>4</sub>]-MWNTs/GCE is estimated to be  $3.3 \text{ mA}\cdot\text{mol}\cdot\text{L}^{-1}\cdot\text{cm}^{-2}$ , which was smaller than that obtained by using GOx-ZnO:Co nanoclusters ( $13.3 \text{ mA}\cdot\text{mol}\cdot\text{L}^{-1}\cdot\text{cm}^{-2}$ ),<sup>48</sup> but larger than that obtained by using PEDOT-Pd/GOx-ME ( $1.6 \text{ mA}\cdot\text{mol}\cdot\text{L}^{-1}\cdot\text{cm}^{-2}$ ).<sup>46</sup>

### Stability and repeatability of the modified electrode

Additional experiments were carried out to test the repeatability and stability. No obvious decrease of the voltammetric response was observed after the GOx-HA-[BMIM][BF<sub>4</sub>]-MWNTs modified electrode was stored in a refrigerator at  $4^\circ\text{C}$  for a week. The electrochemical response of GOx at the modified electrode decreased less than 4% after three weeks. Thus, HA-[BMIM][BF<sub>4</sub>]-MWNTs composite film was very efficient for retaining the activity of GOx. The modified electrode could keep 95% of its initial current response to glucose within three weeks. To estimate the repeatability of the proposed method, the relative standard deviation (RSD) of six times successful measurement of peak current of 0.5 mmol/L glucose was calculated to be 2.4%, which demonstrated the good repeatability of the method.

### Real sample analysis

Practical use of GOx-HA-[BMIM][BF<sub>4</sub>]-MWNTs/GCE was tested by estimating the glucose concentration in human serum sample utilizing standard addition method. The sample was diluted to one-fifth of its concentration using PBS (pH 7). The glucose level was determined to be 0.78 and 0.85 mmol/L at GOx-HA-[BMIM][BF<sub>4</sub>]-MWNTs/GCE. The results obtained at the proposed electrode agreed well with an error value of 2.1%. With an R.S.D. value of 1.8% ( $n = 3$ ), GOx-HA-[BMIM][BF<sub>4</sub>]-MWNTs/GCE is proved to be useful in real sample analysis for the detection of glucose.

### Conclusion

A GOx-HA-[BMIM][BF<sub>4</sub>]-MWNTs/GCE was fabricated. The direct electrochemistry and electrocatalysis behaviors of GOx were investigated at the proposed electrode. The experimental results showed the presence of HA could successfully modify [BMIM][BF<sub>4</sub>]-MWNTs and GOx on the GCE surface, and hinder [BMIM][BF<sub>4</sub>]-MWNTs and GOx leaking from the electrode surface, while revealed that [BMIM][BF<sub>4</sub>]-MWNTs could facilitate the electron transfer between GOx and the basal electrode, and the GOx showed good electrocatalytic activity towards glucose. The proposed electrode was quite stable for at least three weeks. All those suggest that GOx-HA-[BMIM][BF<sub>4</sub>]-MWNTs/GCE is an effective and new third biosensors.

## References

- 1 Feng, J. J.; Xu, J. J.; Chen, H. Y. *J. Electroanal. Chem.* **2005**, *585*, 44.
- 2 Miscoria, S. A.; Barrera, G. D.; Rivas, G. A. *Sens. Actuators B: Chem.* **2006**, *115*, 205.
- 3 Retama, J. R.; Lopez-Ruiz, B.; Lopez-Cabarcos, E. *Biomaterials* **2003**, *24*, 2965.
- 4 Yang, M. H.; Yang, Y. H.; Liu, B.; Shen, G. L.; Yu, R. Q. *Sens. Actuators B: Chem.* **2004**, *101*, 269.
- 5 Li, T.; Yao, Z. H.; Ding, L. *Sens. Actuators B: Chem.* **2004**, *101*, 155.
- 6 Rubio-Retama, J.; Lopez-Cabarcos, E.; Lopez-Ruiz, B. *Talanta* **2005**, *68*, 99.
- 7 Wu, X. J.; Choi, M. M. F. *Anal. Chim. Acta* **2004**, *14*, 219.
- 8 Liu, S. Q.; Leech, D.; Ju, H. X. *Anal. Lett.* **2003**, *36*, 1.
- 9 Baughman, R. H.; Zakhidov, A.; de Heer, W. A. *Science* **2002**, *297*, 787.
- 10 Cai, C. X.; Chen, J. *Anal. Biochem.* **2004**, *332*, 75.
- 11 Davis, J. J.; Coles, R. J.; Hill, H. A. O. *J. Electroanal. Chem.* **1997**, *440*, 279.
- 12 Sun, Y. Y.; Yan, F.; Yang, W. S.; Sun, C. Q. *Biomaterials* **2006**, *27*, 4042.
- 13 Salimi, A.; Sharifi, E.; Noorbakhsh, A.; Soltanian, S. *Biosens. Bioelectron.* **2007**, *22*, 3146.
- 14 Liu, Y.; Wang, M. K.; Zhao, F.; Xu, Z. A.; Dong, S. J. *Biosens. Bioelectron.* **2005**, *21*, 984.
- 15 Liu, Q.; Lu, X. B.; Li, J.; Yao, X.; Li, J. H. *Biosens. Bioelectron.* **2007**, *22*, 3203.
- 16 Salimi, A.; Compton, R. J.; Hallaj, R. *Anal. Biochem.* **2004**, *333*, 49.
- 17 Deng, C. Y.; Chen, J. H.; Chen, X. L.; Xiao, C. H.; Nie, L.; Yao, S. Z. *Biosens. Bioelectron.* **2008**, *23*, 1272.
- 18 Compton, D. L.; Laszlo, J. A. *J. Electroanal. Chem.* **2002**, *520*, 71.
- 19 Zhao, F.; Wu, X.; Wang, M. K.; Liu, Y.; Gao, L. X.; Dong, S. J. *Anal. Chem.* **2004**, *76*, 4960.
- 20 Li, J. W.; Yu, J. J.; Zhao, F. Q.; Zeng, B. Z. *Anal. Chim. Acta* **2007**, *587*, 33.
- 21 Sun, W.; Wang, D. D.; Gao, R. F.; Jiao, K. *Electrochem. Commun.* **2007**, *9*, 1159.
- 22 Safavi, A.; Maleki, N.; Moradlou, O.; Sorouri, M. *Electrochem. Commun.* **2008**, *10*, 420.
- 23 Shangguan, X. D.; Zhang, H. F.; Zheng, J. B. *Electrochem. Commun.* **2008**, *10*, 1140.
- 24 Musameh, M. M.; Kachooangi, R. T.; Xiao, L.; Russell, A.; Compton, R. G. *Biosens. Bioelectron.* **2008**, *24*, 87.
- 25 Wu, X. M.; Du, P.; Wu, P.; Cai, C. X. *Electrochim. Acta* **2008**, *54*, 738.
- 26 Shan, D.; Wang, S. X.; Xue, H. G.; Cosnier, S. *Electrochem. Commun.* **2007**, *9*, 529.
- 27 Zhou, G. J.; Wang, G.; Xu, J. J.; Chen, H. Y. *Sens. Actuators B* **2002**, *81*, 334.
- 28 Guéchet, J.; Edrief, S.; Lasnier, E.; Küper, R. *Immuno-analyse et Biologie Spécialisée* **2008**, *23*, 148.
- 29 Choia, K. Y.; Lee, S.; Park, K.; Kim, K.; Park, J. H.; Kwon, I. C.; Jeong, S. Y. *J. Phys. Chem. Solids* **2008**, *69*, 1591.
- 30 Ma, L.; Tian, Y. N.; Rong, Z. J. *Biochem. Biophys. Methods* **2007**, *70*, 657.
- 31 Liu, H. Y.; Hu, N. F. *J. Phys. Chem. B* **2006**, *110*, 14494.
- 32 Zhang, Y.; Zheng, J. B. *Electrochem. Commun.* **2008**, *10*, 1400.
- 33 Gao, R. F.; Shangguan, X. D.; Qiao, G. J.; Zheng, J. B. *Electroanalysis* **2008**, *20*, 2537.
- 34 Suarez, P. A. Z.; Dullius, J. E. L.; Einloft, S.; De Souza, R. F.; Dupont, J. *Polyhedron* **1996**, *15*, 1217.
- 35 Stoscheck, C. M. *Methods Enzymol.* **1990**, *182*, 50.
- 36 Xue, M. H.; Xu, Q.; Zhou, M.; Zhu, J. J. *Electrochem. Commun.* **2006**, *8*, 1468.
- 37 Park, S. M.; Yoo, J. S. *Anal. Chem.* **2003**, *75*, 455A.
- 38 Feng, J. J.; Zhao, G.; Xu, J.; Chen, H. Y. *Anal. Biochem.* **2005**, *342*, 280.
- 39 Nadzhafova, O.; Etienne, M.; Walcarius, A. *Electrochem. Commun.* **2007**, *9*, 1189.
- 40 Bard, A. J. *Electroanalytical Chemistry*, Marcel Dekker, New York, **1982**, pp. 53–157.
- 41 Laviron, E. *J. Electroanal. Chem.* **1979**, *100*, 263.
- 42 Laviron, E. *J. Electroanal. Chem.* **1979**, *101*, 19.
- 43 Sheng, Q. L.; Shen, Y.; Zhang, H. F.; Zheng, J. B. *Chin. J. Chem.* **2008**, *26*, 1244.
- 44 Liu, S. Q.; Ju, H. X. *Biosens. Bioelectron.* **2003**, *19*, 177.
- 45 Liu, Q.; Lu, X. B.; Li, J.; Yao, X.; Li, J. H. *Biosens. Bioelectron.* **2007**, *22*, 3203.
- 46 Santhosh, P.; Manesh, K. M.; Uthayakumar, S.; Komathi, S.; Gopalan, A. I.; Lee, K.-P. *Bioelectrochemistry* **2009**, *75*, 61.
- 47 Shu, F. R.; Wilson, G. S. *Anal. Chem.* **1976**, *48*, 1679.
- 48 Zhao, Z. W.; Chen, X. J.; Tay, B. K.; Chen, J. S.; Han, Z. J.; Khor, K. A. *Biosens. Bioelectron.* **2007**, *23*, 135.
- 49 Rogers, M. J.; Brandt, K. G. *Biochemistry* **1971**, *10*, 4624.
- 50 Amine, A.; Kauffmann, J. M.; Guilbault, G. G. *Anal. Lett.* **1993**, *26*, 1281.
- 51 Vidal, J. C.; Garcia, E.; Castillo, J. R. *Biosens. Bioelectron.* **1998**, *13*, 371.

(E1003172 Cheng, F.; Lu, Y.)